

# Nonlinear dynamics, rectification, and phase locking for particles on symmetrical two-dimensional periodic substrates with dc and circular ac drives

C. Reichhardt, C.J. Olson Reichhardt, and M.B. Hastings

*Center for Nonlinear Studies and Theoretical Division, Los Alamos National Laboratory, Los Alamos, New Mexico 87545*  
(April 17, 2021)

We investigate the dynamical motion of particles on a two-dimensional symmetric periodic substrate in the presence of both a dc drive along a symmetry direction of the periodic substrate and an additional circular ac drive. For large enough ac drives, the particle orbit encircles one or more potential maxima of the periodic substrate. In this case, when an additional increasing dc drive is applied in the longitudinal direction, the longitudinal velocity increases in a series of discrete steps that are integer multiples of  $a\omega/(2\pi)$ , where  $a$  is the lattice constant of the substrate. Fractional steps can also occur. These integer and fractional steps correspond to distinct stable dynamical orbits. A number of these phases also show a rectification in the positive or negative transverse direction where a non-zero transverse velocity occurs in the absence of a dc transverse drive. We map out the phase diagrams of the regions of rectification as a function of ac amplitude, and find a series of tongues. Most of the features, including the steps in the longitudinal velocity and the transverse rectification, can be captured with a simple toy model and by arguments from nonlinear maps. We have also investigated the effects of thermal disorder and incommensuration on the rectification phenomena, and find that for increasing disorder, the rectification regions are gradually smeared and the longitudinal velocity steps are no longer flat but show a linearly increasing velocity.

PACS numbers: 05.60.-k, 05.45.-a, 74.25.Qt, 87.16.Uv.

## I. INTRODUCTION

Recently there has been a growing interest in nonequilibrium systems that show a rectification or ratchet effect, typically for a particle moving in some form of asymmetric potential [1]. In these systems, a net dc drift in one direction can occur even though only an ac drive or ac flashing of the potential is applied. Such ratchet phenomena have been examined in a variety of systems, including biological motors [2], colloidal particles moving through asymmetric potentials [2,3], atom transport in optical lattices [4], charge transport in quantum dot systems [5], transport of granular particles [6], and vortices in superconductors and SQUIDs [7,8]. In most of these systems there is some form of underlying asymmetric substrate potential which is responsible for the symmetry breaking that gives rise to the rectification. Additionally, most of the systems studied so far have one-dimensional (1D) or effectively 1D geometries.

For 2D systems, it is possible to break the symmetry of the system without introducing an asymmetric substrate. One example of rectification in 2D is the motion of biomolecules or polymers through periodic arrays of posts [9,10]. Here the particles are driven in alternating directions by an electric field. Another approach to 2D rectification is to drive particles through a periodic array at various angles [11–13]. The particle motion becomes locked to certain stable angles, such as  $45^\circ$  for a square array, even when the external drive is applied in a different direction. Several theoretical studies have also considered models of particles moving in 2D asymmetric

potentials, leading to rectification and negative differential conductivity [14,15]. In a recently proposed model, spatiotemporal symmetry breaking is caused by the application of an external wave to a system with a periodic potential [16]. In other models, the asymmetry of quantities other than the substrate produces a rectification [17]. A better understanding of 2D systems that exhibit rectification can assist in the creation of technological devices for applications such as the separation of different species of colloids or biomolecules or new techniques for electrophoresis.

The phase locking that occurs when particles are driven over periodic substrates in the presence of an ac drive has also been intensely studied. This phenomenon arises when the external ac frequency  $\omega$  matches the internally generated frequency of the motion of the particle over the periodic potential. One of the best known examples of phase locking is the Shapiro steps observed as steps in the  $V(I)$  curves of Josephson-junction arrays [18]. The step widths oscillate with the ac amplitude  $A$ , with the  $n$ th step varying as the modified Bessel function  $J_n(A/\omega)$ . Shapiro step-like phase locking is also observed for dc and ac drives in sliding charge-density wave systems [19], as well as vortex motion in superconductors with periodic substrates [20–22].

In typical phase-locking systems, the ac drive is applied in the *same* direction as the dc drive. Additionally, most of the well-studied phase locking systems can be considered as effectively 1D. Phase locking should also occur in 2D when the ac drive is applied in a different direction from the dc drive; however, very little is known about

the behavior of phase locking in this case. Rectification may occur even for motion in a symmetric potential if the ac drive in a 2D system breaks the symmetry, such as a circular ac drive.

In a recent model for vortices in a 2D superconductor moving over a periodic potential, the ac drive was *perpendicular* to the dc drive [23]. In this case the phase locking that occurred was distinct from Shapiro steps. For these perpendicular ac drives, the widths of the steps do not oscillate with the drive amplitude, as would be expected for Shapiro steps, but instead they monotonically increase as the square of the ac amplitude for square substrates and linearly for triangular substrates.

For elastic media moving over a *random* substrate, it is also possible to have a periodic velocity component in both the longitudinal and transverse directions due to the periodicity of the elastic media itself. When an ac drive is applied in the same direction as the dc drive for random disorder, Shapiro-like phase locking effects can again be observed, such as in sliding charge density waves [19] and vortex lattices [24–26]. In recent simulations and theory for the case of a perpendicular ac drive for vortex lattices interacting with random pinning, a transverse phase locking occurs [27]. In 2D, it is possible to apply *two* ac drives which are perpendicular to one another such that the particle, in the absence of a dc drive, would move in a circle. The behavior of the system in this case has been largely unexplored.

In this work we study the motion of overdamped particles moving over a two-dimensional symmetric periodic substrate where there are two perpendicular ac drives and an additional dc drive that is applied along a symmetry direction of the substrate. In Section II we outline our model and the simulation technique. In Section III, we show that for small ac amplitudes and low dc drives, the particle moves in a circular orbit near the potential minimum. As a function of the applied dc driving force  $f_{dc}$  in the longitudinal direction, there is a depinning threshold for the particle motion. For increasing drive beyond the threshold, the longitudinal velocity  $V_x$  increases in a series of steps; however, there is no rectification and the transverse velocity  $V_y$  is zero. For increasing ac amplitude of fixed frequency and no dc drive, the circular particle orbit increases in radius, and there are a series of stable orbits which are commensurate with the periodicity of the substrate. In Section IV, we illustrate that when a dc drive is applied for ac amplitudes such that the particle orbit encircles one potential maximum, the longitudinal velocity again increases in a series of prominent integer steps. Between these integer steps, there are a series of smaller fractional steps with a structure similar to a Devil’s staircase. In Section V, we show that for the same range of ac amplitude where the particle orbit encircles one maximum, there are also distinct regions where a transverse rectification occurs. The rectification phases are centered between the integer steps in

the longitudinal velocity. The maximum velocity in the rectification regions is  $a\omega/(2\pi)$ , and we observe smaller fractional rectification steps as well. The rectification can be in either the positive or negative direction. We map out the phase diagram of the rectification phases as a function of ac amplitude and dc drive, and show that it consists of a series of tongues. We find in general that as the ac amplitude increases, the number of regions that show a rectification also increases. In Section VI we examine the effects of disorder. For increasing thermal disorder, the phases begin to smear; however, regions of rectification persist up to high temperatures. We also consider the effects of particle-particle interactions when multiple particles move through the arrays. In this case, incommensuration effects produce a partial smearing of the phases. In Section VII we examine a simple model that captures most of the features of the system, including integer and fractional steps in the longitudinal velocity as well as steps in the transverse velocity that correspond to positive or negative rectification. In Section VIII we discuss some experimental systems in which the phase locking and ratchet effects might be observed, including colloids moving through periodic traps, biomolecules driven through arrays of posts, vortices in superconductors with periodic pinning arrays, and classical electron motion in antidot arrays. A shorter version of portions of the work presented here has been previously published [28].

## II. SIMULATION

We consider an overdamped particle moving in two dimensions and interacting with an underlying square periodic substrate, where we use periodic boundary conditions in the  $x$  and  $y$  directions. The equation of motion for a particle  $i$  is

$$\mathbf{f}_i = \mathbf{f}_s + \mathbf{f}_{dc} + \mathbf{f}_{ac} = \eta \mathbf{v}_i, \quad (1)$$

where the damping constant  $\eta$  is set to unity. The substrate force,  $\mathbf{f}_s$ , arises from a square array with period  $a$  of repulsive sites, each of which has force  $\mathbf{f}_s^j = -\nabla U(r)$ . To model specific physical systems we consider  $U(r) = \ln(r)$ , corresponding to a thin film superconductor with a periodic array of pinning sites, where each pinning site captures one vortex and an additional vortex sits in the interstitial region between pinning sites. This interstitial vortex interacts with a square periodic substrate created by the pinned vortices. We have also considered  $U(r) = 1/r$  and  $U(r) = e^{-r\kappa}/r$ , which could model one mobile particle in an array of trapped colloids or ions. We have considered systems of different sizes and find that for most of the results presented here,  $8a \times 8a$  is adequate. The dc drive  $\mathbf{f}_{dc}$  is applied along the symmetry axis of the substrate array, in the  $x$  or longitudinal direction. The ac drive has two components, given by

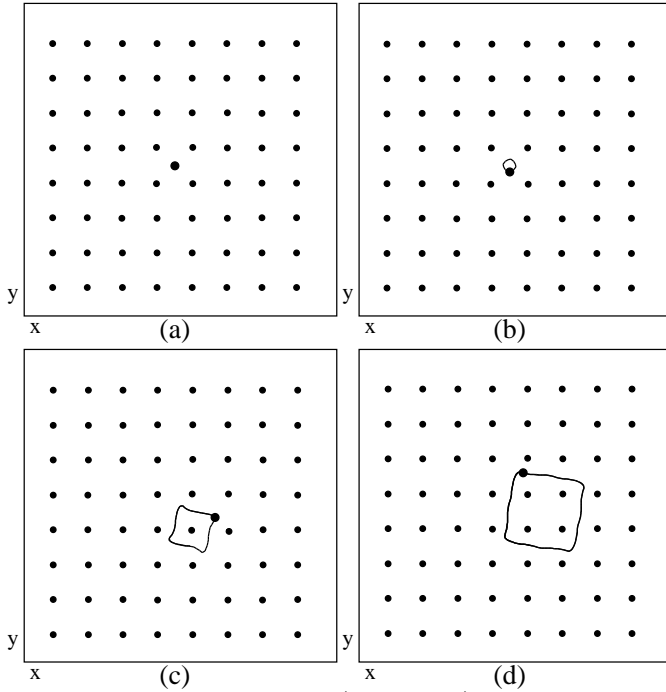


FIG. 1. Potential maxima (black dots), driven particle (large dot), and particle trajectory (black line) for ac amplitude  $A =$  (a) 0.0, (b) 0.15, (c) 0.3, and (d) 0.45.

$$\mathbf{f}_{ac} = A \sin(\omega_A t) \hat{\mathbf{x}} - B \cos(\omega_B t) \hat{\mathbf{y}}. \quad (2)$$

In all of our results there is *no* dc driving component in the  $y$  or transverse direction. We fix  $w_A/w_B = 1.0$  and  $A = B$ . As an initial condition, we place the particle close to the center of a plaquette. For different initial placements, the results are identical. In a single simulation the dc drive  $f_{dc}$  is increased from 0 to 2.0 in increments of 0.0001, where  $3 \times 10^5$  time steps are spent at each increment to ensure a steady state. We measure the particle trajectories and velocities in the longitudinal  $V_x = \sum_i^{N_v} \hat{\mathbf{x}} \cdot \mathbf{v}_i$  and transverse direction  $V_y = \sum_i^{N_v} \hat{\mathbf{y}} \cdot \mathbf{v}_i$ . We have also considered the cases  $A \neq B$  and  $\omega_A \neq \omega_B$ , as well as the addition of a phase offset and driving with more complicated ac forms. These introduce a considerable number of new behaviors not found for the strictly circular case, and have been detailed in a separate publication [29].

### III. COMMENSURATE ORBITS AND DEPINNING

In Fig. 1 we show the locations of the substrate potential maxima of the form  $\ln(r)$  and the trajectories or orbits of the mobile particle for fixed  $f_{dc} = 0.0$  and ac amplitudes of  $A =$  (a) 0.0, (b) 0.15, (c) 0.3 and (d) 0.45. For  $A = 0$  [Fig. 1(a)], the particle is stationary and is located at the center of a plaquette at the potential minimum. For  $0.0 < A < 0.25$ , the particle moves

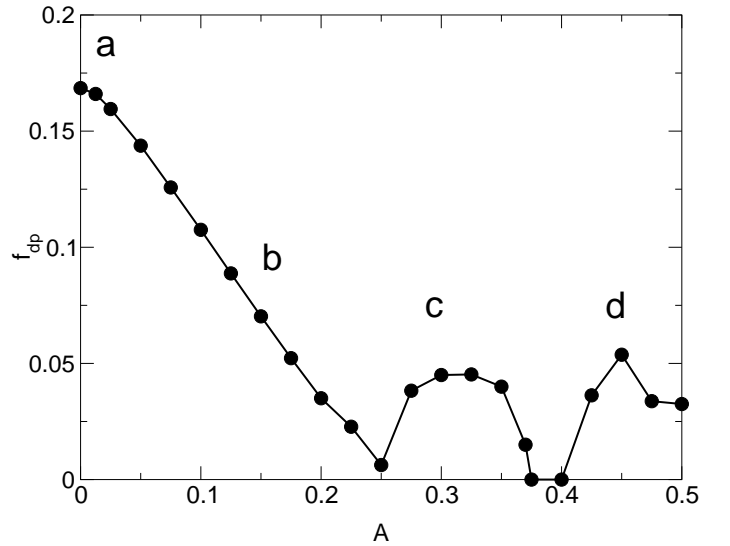


FIG. 2. Depinning force  $f_{dp}$  vs ac amplitude  $A$ . The letters a, b, c, and d correspond to the amplitudes at which the orbits shown in Fig. 1(a-d) occur.

in a circular orbit around the center of the plaquette, as seen in Fig. 1(b). The radius of the orbit increases with  $A$ , and the orbit becomes increasingly square as  $A$  approaches 0.25, reflecting the square symmetry of the caging potential in the plaquette. For  $0.25 < A < 0.375$ , the radius of the orbit is large enough that, during a single periodic cycle, the particle encircles one potential maximum, as shown in Fig. 1(c). For  $0.4 < A < 0.5$ , the particle moves in a stable orbit that encircles four potential maxima, as in Fig. 1(d). Between the regions where four and one maxima are encircled, for  $0.375 < A < 0.4$ , the orbits are unstable and the particle is no longer localized but undergoes diffusion. Stable orbits also occur for higher ac amplitudes where 9 and 25 maxima are encircled, with regions of delocalized particle motion falling between the ac amplitudes that produce stable orbits. A similar phenomena of commensurate orbits for particles undergoing circular or cyclotron motion in a periodic array of scatterers also occurs in electron pinball models [30]. Another similar system is the vortex pinball model, where stable orbits occur for vortices in superconductors with periodic pinning arrays when the density of the magnetic field is such that there are twice as many vortices as pinning sites [31].

In Fig. 2 we plot the depinning threshold  $f_{dp}$  vs ac amplitude  $A$  for the system in Fig. 1 under the application of a dc force. The depinning threshold decreases continuously with increasing  $A$  for  $0.0 < A < 0.25$  when the particle is circling inside a single plaquette, as illustrated in Fig. 1(b). For  $A > 0.25$ , the depinning threshold increases with  $A$  and reaches a local maximum at  $A = 0.3$ , corresponding to the center of the range of ac amplitudes over which the stable orbit encircles one potential maximum [Fig. 1(c)]. The depinning threshold drops to zero for  $0.375 < A < 0.4$ , when the particle is delocalized. For

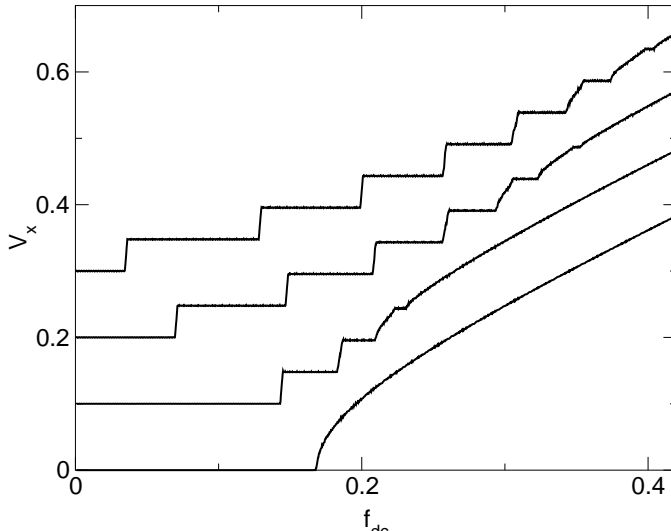


FIG. 3. The velocity in the  $x$ -direction,  $V_x$ , vs  $f_{dc}$  for  $A = 0.0, 0.05, 0.15$ , and  $0.2$  from bottom to top. The curves have been systematically shifted in  $y$  for clarity.

$A > 0.4$ ,  $f_{dp}$  again increases with  $A$  to a local maximum at  $A = 0.45$  at the center of the region where the particle orbit encircles four potential maxima. We also find non-zero depinning thresholds for higher values of  $A$  at which 9 and 25 potential maxima are encircled by the orbit in a single period.

#### IV. PHASE LOCKING FOR LOW AC AMPLITUDES

We now consider the phase locking phenomena for low ac amplitudes  $0 < A < 0.25$ , when the particle moves in the interstitial region between the potential maxima as in Fig. 1(b). In Fig. 3 we plot  $V_x$  vs  $f_{dc}$  for increasing ac amplitudes  $A = 0.0, 0.05, 0.15$ , and  $0.2$ , showing that a series of steps occur which increase in width with increasing  $A$  from zero at  $A = 0$ . The depinning threshold decreases with increasing  $A$ . The height of the  $n$ th step is  $V_x = n a \omega / (2\pi)$ , and as  $A$  increases, higher order steps can be resolved. If the ac drive were applied in the  $x$ -direction only, Shapiro-type steps would occur with  $V_x = n a \omega / (2\pi)$  on the  $n$ th step. For Shapiro type phase locking, the velocity vs force curve at the beginning and end of each step would be continuous; however, the edges of the steps in Fig. 3 are extremely sharp. The average velocity component in the  $y$ -direction is strictly zero for all values of  $A < 0.25$ . For varied  $\omega$  the location of the steps shifts; however, the same general behavior occurs.

The quantization of the step height is a result of the periodicity of the drive. Although the particle has translated by  $n$  unit cells in the  $x$ -direction after a single period of the drive, the particle is in the *same location* within its unit cell as it was at the start of the period. Thus, up to this translation by  $n$  cells, the orbit is

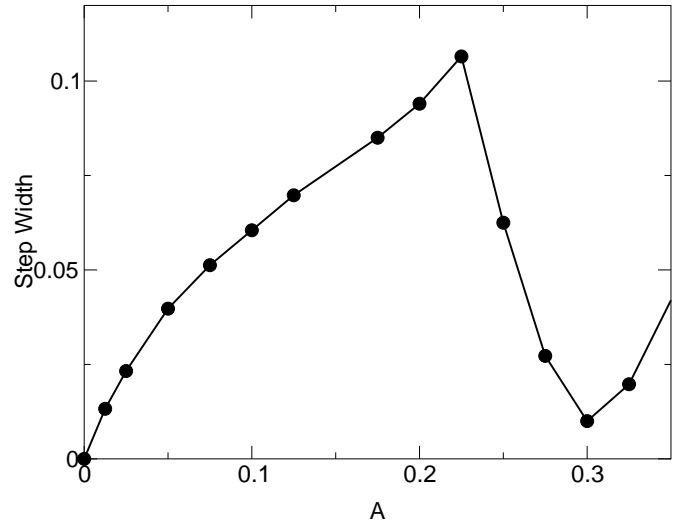


FIG. 4. Width of the the first phase locking step  $n = 1$  vs  $A$  from the curves shown in Fig. 3.

periodic with period  $2\pi/\omega$ . The particle therefore moves a distance of  $na$  in a time of  $2\pi/\omega$ , giving a velocity of  $V_x = n a \omega / (2\pi)$ .

In Fig. 4 we plot the width  $W$  of the  $n = 1$  step vs  $A$  for  $0.0 < A < 0.36$ . The width increases with  $A$  for  $A < 0.225$ , an ac amplitude just below the transition at which the particle orbit changes from encircling zero to encircling one potential maximum at zero dc drive.  $W$  then decreases with increasing  $A$ , reaching a minimum at  $A = 0.3$ , which corresponds to the peak in the depinning threshold shown in Fig. 2. For Shapiro step-type locking, the higher order step widths would fit to a Bessel function as a function of ac amplitude. Here, although the step width  $W$  does show an oscillatory behavior similar to that of Shapiro steps,  $W$  does not fit well to a Bessel function form, particularly due to the sharp cusp at  $A = 0.225$ .

In Fig. 5(a,b) we illustrate the particle trajectories along the first and second steps in  $V_x$  for fixed  $A = 0.15$ , and in Fig. 5(c) we show an orbit for a non-step region. Along the  $n = 1$  step (Fig. 5(a)), the particle performs a loop at the center of each plaquette and its motion is perfectly regular. For the  $n = 2$  step (Fig. 5(b)), the regular particle orbit has a kink or very small loop in every second plaquette. For higher order steps, we find stable orbits similar to those shown in Fig. 5(a,b), where for the  $n$ th step a small loop in the orbit occurs in every  $n$ th plaquette. For a typical non-step region, such as that illustrated in Fig. 5(c), the orbits are disordered or chaotic, and the particle does not follow any particular trajectory. We also find that some fractional steps can occur near the edges of the main steps with  $V_x = p a \omega / (2\pi q)$ , where  $p$  and  $q$  are integers. These fractional steps are much smaller in width than the integer steps.

The origin of the fractional steps is similar to that of the integer steps. Consider a particle that has started in

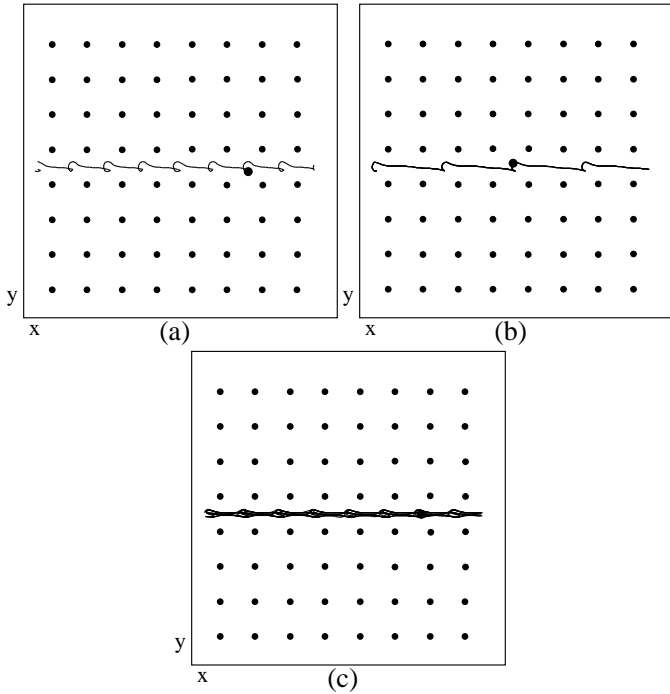


FIG. 5. Potential maxima (black dots), driven particle (large dot), and particle trajectories (black lines) for the sample in Fig. 3 at  $A = 0.15$ . (a) The particle orbit on the  $n = 1$  step in  $V_x$  at  $f_{dc} = 0.1$ . (b) The orbit for the  $n = 2$  step at  $f_{dc} = 0.17$ . (c) The particle orbit for the non step region at  $f_{dc} = 0.208$ .

a given position within some unit cell. After a single period of the drive, the particle may or may not have moved to another cell. However, after a single period, it is in a *different* position within the unit cell than that which it occupied at the start. Only after  $q$  periods elapse does the particle return to the same position in the unit cell. Thus, up to a translation by some number of unit cells, the orbit is periodic with period  $2\pi q/\omega$ . If the particle translates by  $p$  cells in this time, we obtain a velocity of  $V_x = pa\omega/(2\pi q)$ .

## V. PHASE LOCKING AND RECTIFICATION FOR HIGHER AC AMPLITUDES

We next turn to the phase locking for ac amplitudes  $0.225 < A < 0.4$ , where the particle orbit encircles one potential maximum as shown in Fig. 1(c). In Fig. 6 we plot  $V_x$  vs  $f_{dc}$  for increasing ac amplitudes of  $A = 0.25, 0.275, 0.3, 0.325, 0.35, 0.375$ , and  $0.4$ . Fig. 6 shows that  $V_x$  exhibits a series of steps, most of which have  $dV_x/df_{dc} = 0$ . The  $n$ th step has  $V_x = na\omega/(2\pi)$ . For increasing ac amplitudes, more steps can be resolved at higher values of  $f_{dc}$ . The widths of some of the steps can be seen to grow with increasing  $A$ , while others decrease. There are also some regions of drive which do not

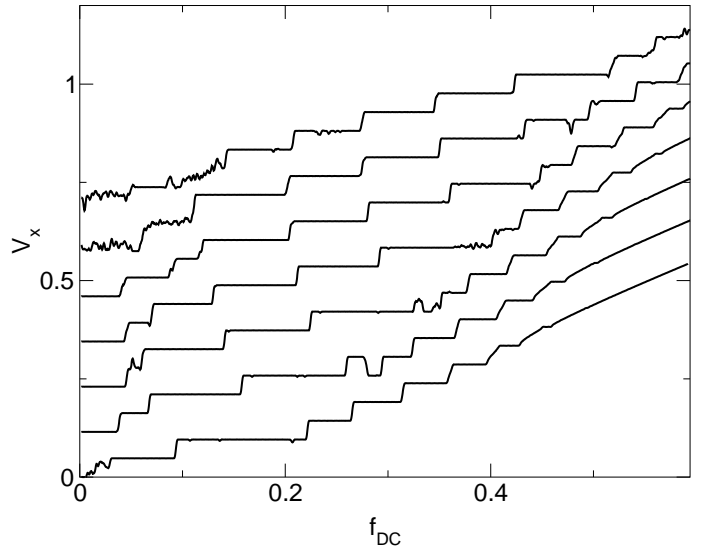


FIG. 6.  $V_x$  vs  $f_{dc}$  for, from bottom to top,  $A = 0.25, 0.275, 0.3, 0.325, 0.35, 0.375$ , and  $0.4$ . The curves have been systematically shifted in  $y$  for clarity.

settle onto clearly defined steps. These regions become more prominent for higher values of  $A$ . For example, in Fig. 6, the depinning and the  $n = 1$  and  $2$  steps of the two upper curves  $A = 0.375$  and  $0.4$  have large fluctuations. The depinning threshold for the bottom curve at  $A = 0.25$  also shows a similar behavior. These values of  $A$  are close to or at the transition where the number of potential maxima encircled by the particle orbit at  $f_{dc} = 0.0$  changes. For the upper curves, this is from one to four maxima, and for the lower curve, it is from zero to one maximum. By watching animations of the particle orbits, we observe that in general the particle is jumping between the two different orbits on these poorly defined steps. At these values of  $A$  the particle orbits are delocalized and the depinning threshold is zero, as shown in Fig. 2. Another feature of the  $V_x$  curves is that occasionally there are regions where the velocity jumps down in value with increasing  $f_{dc}$ , such as in the  $A = 0.275$  curve near the transition between the  $n = 3$  and  $n = 4$  steps at  $f_{dc} = 0.28$ . In these cases the particle orbit jumps from the higher  $n$  orbit back to the lower state. In general these step down effects occur near the  $n$  to  $n + 1$  transitions. If we repeat the same simulation with slightly different initial conditions, similar jumps occur in the same regions of  $f_{dc}$  but are not identical. We have previously shown that along the flat steps, the particle orbits are stable. Along the  $n$ th step the particle moves a distance  $na$  in the  $x$  direction in a single period.

In Fig. 7 we show the particle orbits on the integer steps  $n = 1, 2, 3$ , and  $4$  for the system in Fig. 6 at  $A = 0.325$ . For the drives shown,  $\langle V_y \rangle = 0$ . At zero drive, the orbit has the square shape illustrated in Fig. 1(c). On the  $n = 1$  step at  $f_{dc} = 0.054$  (Fig. 7(a)), the particle circles around a single maximum and moves in the  $x$  direction by a distance  $a$  per period. For the

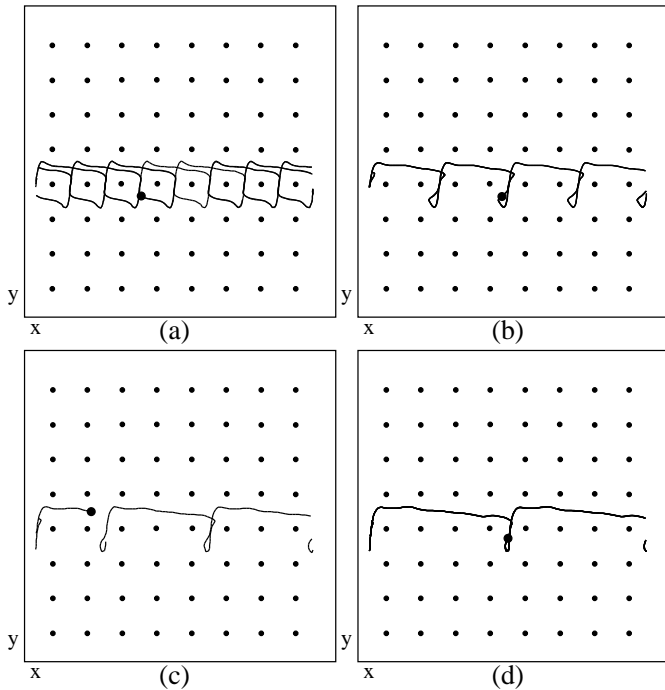


FIG. 7. Particle trajectories (black lines), driven particle (large dot), and periodic potential maxima (black dots) for the first four steps in  $V_x$  from Fig. 6 for the  $A = 0.325$  curve. (a)  $n = 1$  step at  $f_{dc} = 0.054$ . (b)  $n = 2$  step at  $f_{dc} = 0.1$ . (c)  $n = 3$  step at  $f_{dc} = 0.18$ . (d)  $n = 4$  step at  $f_{dc} = 0.24$ .

$n = 2$  step at  $f_{dc} = 0.1$  (Fig. 7(b)), the nature of the particle motion changes. Rather than circling around every second maximum, the particle moves through a smaller loop that is less than  $a$  in diameter in every other plaquette so that in one period the particle moves a distance  $2a$ . Similar motion occurs on the  $n = 3$  step at  $f_{dc} = 0.18$  (Fig. 7(c)), but the loop occurs every third plaquette. Along the  $n = 4$  step at  $f_{dc} = 0.24$  (Fig. 7(d)), the particle translates  $4a$  in a single period.

In Fig. 8 we plot the orbits along the  $n = 5, 7, 8,$  and  $9$  steps for the same system as in Fig. 6 at  $A = 0.325$ . For the  $n = 5$  step at  $f_{dc} = 0.325$ , the orbit is essentially the same as those in steps  $n = 2$  to  $n = 4$  from Fig. 7. The figure has a loop in every plaquette since we have shown the particle crossing the periodic boundary several times, and the particle does not follow its previous path until it has completed several passes through the system due to the fact that the orbit repeats every five plaquettes but the sample has an even number of plaquettes. If we chose a system size which is a multiple of  $5a$  wide, the orbit is repeated during each pass through the system. Whether the sample size is commensurate with the orbit shape does not change any features in  $V_x$  or  $V_y$ . On the  $n = 7$  step at  $f_{dc} = 0.45$  (Fig. 8(b)), the particle is moving fast enough in the  $x$  direction that it can no longer loop down into the lower row. The orbit still shows a small loop inside the row every seventh plaquette. For the  $n = 8$  step shown in Fig. 8(c) at  $f_{dc} = 0.49$ , the particle

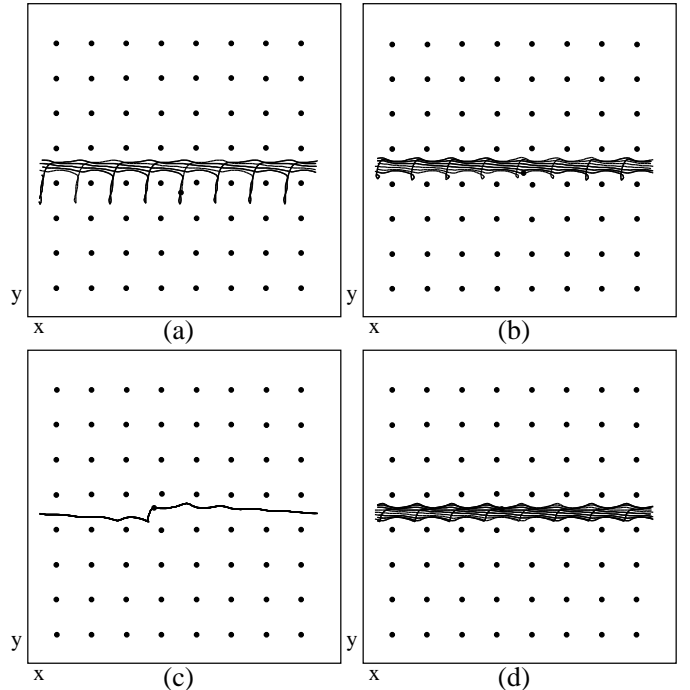


FIG. 8. Particle trajectories (black lines), periodic potential maxima (black dots), and driven particle (large dot) for the velocity steps from Fig. 6 at  $A = 0.325$ . (a)  $n = 5$  step at  $f_{dc} = 0.325$ . (b)  $n = 7$  step at  $f_{dc} = 0.45$ . (c)  $n = 8$  step at  $f_{dc} = 0.49$ . (d)  $n = 9$  step at  $f_{dc} = 0.53$ .

motion is again contained within one row and shows a very small loop every  $8a$ . The orbit is commensurate with the sample size so the orbit repeats exactly during each pass. For the  $n = 9$  step at  $f_{dc} = 0.53$  (Fig. 8(d)), the orbit is similar to that seen for the  $n = 7$  and  $n = 8$  steps, with a small loop every  $9a$ . For much higher  $f_{dc}$ , the particle does not lock to a fixed orbit for this value of  $A$ .

In addition to the integer steps, we also observe fractional steps in the regions between the integer steps. In general these fractional phases are associated with the onset of rectification, where the average particle velocity is no longer strictly in the  $x$  direction.

### A. Rectifying Phases

In Fig. 9 we plot simultaneously  $V_x$ , which increases with  $f_{dc}$ , and  $V_y$  vs  $f_{dc}$  for a fixed value of  $A = 0.325$ . Here, the steps in  $V_x$  have height  $a\omega/(2\pi)$ , while  $V_y$  shows *non-zero values* centered at the step transitions in  $V_x$ . The maximum value of  $V_y$  is  $a\omega/(2\pi)$  in the positive direction as seen near the  $n = 2$  to  $n = 3$ ,  $n = 3$  to  $n = 4$ , and  $n = 4$  to  $n = 5$  step transitions. At the  $n = 5$  to  $n = 6$  transition,  $V_y = -a\omega/(2\pi)$ . There are also ranges of drive over which the value of  $V_y$  is not a multiple of  $a\omega/(2\pi)$ , such as at the  $n = 0$  to  $n = 1$ ,  $n = 1$  to  $n = 2$ , and the  $n = 5$  to  $n = 6$  steps. Rectification occurs

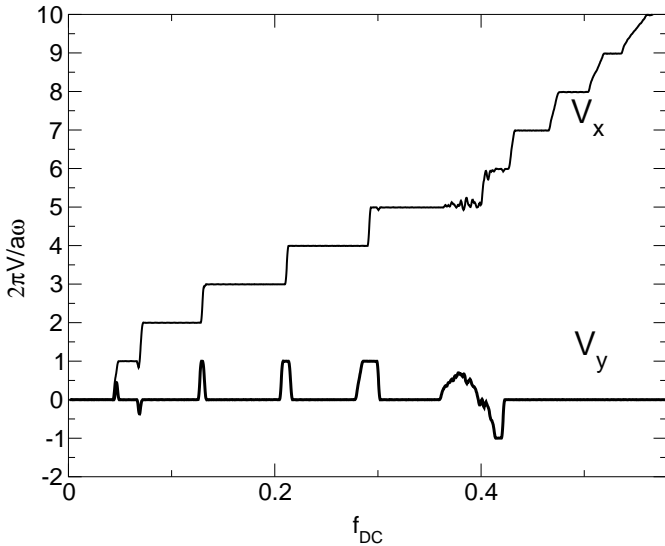


FIG. 9.  $V_x$  (light line) and  $V_y$  (dark line) vs  $f_{dc}$  for  $A = 0.325$ .

everywhere along the  $n = 6$  step. No rectification occurs for the  $n = 7$  step and above, which also corresponds to the orbits becoming confined to a single row for these high  $f_{dc}$  values, as illustrated in Fig. 8.

The rectification can be understood by considering the symmetries of the problem. The dc drive breaks the reflection symmetry across the  $y$ -axis,  $R_y$ , but preserves  $R_x$ , reflection across the  $x$ -axis, as can be seen by noting that the reflection  $R_y$  would change the sign of the dc drive (which is applied in the  $x$ -direction) while the reflection  $R_x$  would leave the drive unchanged. The dc drive also breaks the combined symmetry  $R_x R_y$ . The ac drive breaks both  $R_x$  and  $R_y$  individually, but preserves the combined symmetry  $R_x R_y$ . Here, either the reflection  $R_x$  or the reflection  $R_y$  reverse the direction of the ac drive from counter-clockwise to clockwise, but the combination  $R_x R_y$  leaves the drive unchanged up to a change in the phase of the drive (corresponding to a shift in  $t$  by half a period). The combination of the ac and dc drives break all of the symmetries in the problem.

To see the effect of the symmetries, consider first the situation with only the dc drive, when the system has the symmetry  $R_y$ . Then, if the particle has an orbit with non-zero  $V_y$ , by symmetry it must also have an orbit with the opposite  $V_y$ . If both such orbits exist, there is a spontaneous symmetry breaking which can produce a rectification. Such a spontaneous symmetry breaking has been observed in similar systems [32]. Similarly, if we have only the ac drive, the system has the symmetry  $R_x R_y$ . Then the existence of an orbit with given  $V_x, V_y$  would imply the existence of an orbit with velocities  $-V_x, -V_y$ , and spontaneous symmetry breaking would again be possible. In the case considered in our simulations, since *all* symmetries are broken, we can have rectifying orbits *without* any spontaneous symmetry breaking. We have seen in fact that the sign of the rectification does not

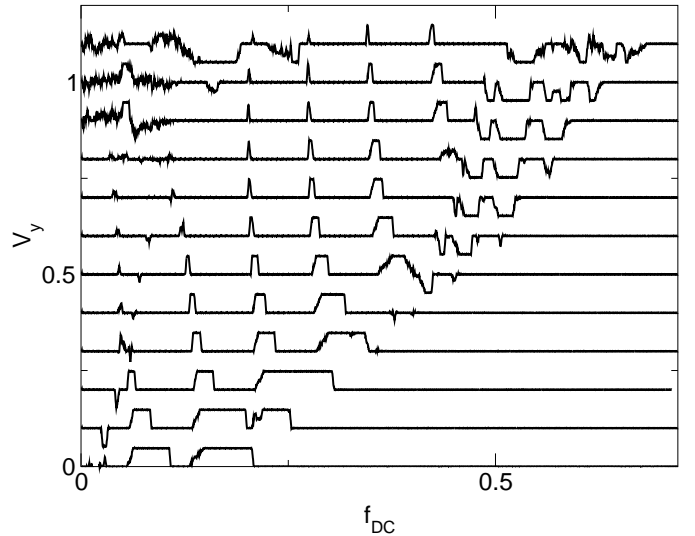


FIG. 10. Velocity in the  $y$ -direction,  $V_y$ , vs  $f_{dc}$  for  $A = 0.25, 0.262, 0.28, 0.306, 0.31, 0.327, 0.343, 0.356, 0.363, 0.375, 0.38$ , and  $0.4$ , from bottom to top. There is a systematic shift in the  $y$ -direction added for clarity.

depend on initial conditions, and we show below that the rectification persists even at non-zero temperature; both of these are consequences of the fact that the symmetries of the system are broken by the drives, rather than broken spontaneously.

In Fig. 10 we plot a series of  $V_y$  vs  $f_{dc}$  curves for  $0.25 \leq A \leq 0.4$ , showing the evolution of the rectifying regions. As  $A$  increases, the maximum value of  $f_{dc}$  at which rectification is observed also increases, coinciding with the resolution of more integer steps as shown in Fig. 6. For  $A < 0.32$  (the first five curves from the bottom), the rectification is predominantly in the positive  $y$  direction, while for  $A > 0.32$ , several phases appear which rectify in the negative  $y$  direction, as seen for  $A = 0.327, 0.343, 0.356$ , and  $0.363$ . For  $A > 0.37$  (the top three curves), an increasing number of regions appear where there is no well defined locking but there is some form of rectification. These disordered regions first occur at low  $f_{dc}$  values for  $A = 0.375$  and  $0.38$ , while for the  $A = 0.4$  curve the disordered regions also appear at higher  $f_{dc} = 0.6$ . The rectification phases shift in position with  $A$  and the width of the phases grows and then subsequently shrinks with  $A$ . The phases which rectify in the positive direction shift toward lower  $f_{dc}$  with increasing  $A$ , while the negative rectification phases shift toward higher  $f_{dc}$  as  $A$  is increased. The shift can be qualitatively understood by considering that the particle rotates clockwise. For the positive rectification regions, if we consider one cycle starting at a position of  $y = a/2$  and  $x = 0$  and circling around the potential maximum at  $(0, 0)$ , the particle is moving fastest near  $y = +a/2$  when the ac and dc drives are in the same direction, and slowest near  $y = -a/2$  when the ac drive opposes the force from the dc drive. If, on the  $n$ th step, the particle

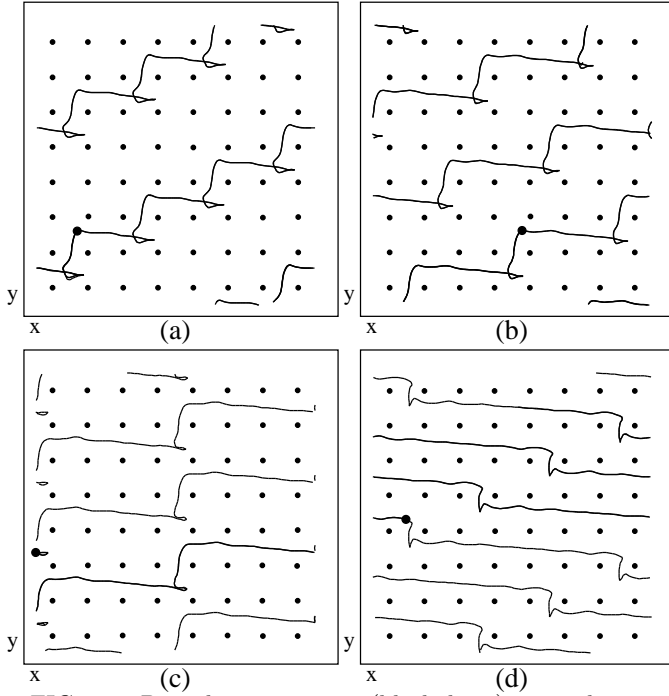


FIG. 11. Particle trajectories (black lines), periodic potential maxima (black dots), and driven particle (large dot), showing integer rectifying orbits from the system in Fig. 9 for  $A = 0.325$  and  $f_{dc} =$  (a) 0.1295, (b) 0.21, (c) 0.29, and (d) 0.42.

translates a distance  $na$  per period, then on the downward moving portion of the ac orbit, the particle interacts strongly with one of the potential maxima. If this interaction is too strong, the particle cannot translate down by one row in the  $y$  direction. At the same time, the particle continues to move in the positive  $x$  direction. If, during the downward stroke, the particle moves a distance close to  $na/2$ , then on the upward part of the ac cycle, the particle does *not* interact strongly with a potential maximum and can thus move up in the  $y$  direction by a distance  $a$ . As a result, there is a net motion in the  $+y$  direction each cycle. The positions of the positive rectifying regions shift to lower  $f_{dc}$  at higher values of  $A$  since, in the portion of the cycle when the ac and dc forces are in the same direction, a smaller dc drive is required to translate the particle a distance  $na$  for larger  $A$ . We also note that if the circular ac drive is reversed, the  $V_y$  vs  $f_{dc}$  curves are flipped and positive rectification becomes negative rectification.

In Fig. 11 we show several examples of rectifying phases where  $V_y = a\omega/(2\pi)$  for the case of  $A = 0.325$  from Fig. 9. Figure 11(a) illustrates the first integer rectifying phase for  $f_{dc} = 0.1295$  where there is a transition from the  $n = 2$  to the  $n = 3$  step. In a single cycle, the particle moves  $2a$  in the  $x$  direction and  $a$  in the  $y$  direction. Additionally, a small loop in the orbit occurs in every third plaquette. Similar motion occurs on the  $n = 3$  step at larger  $f_{dc}$ , where the particle moves  $3a$

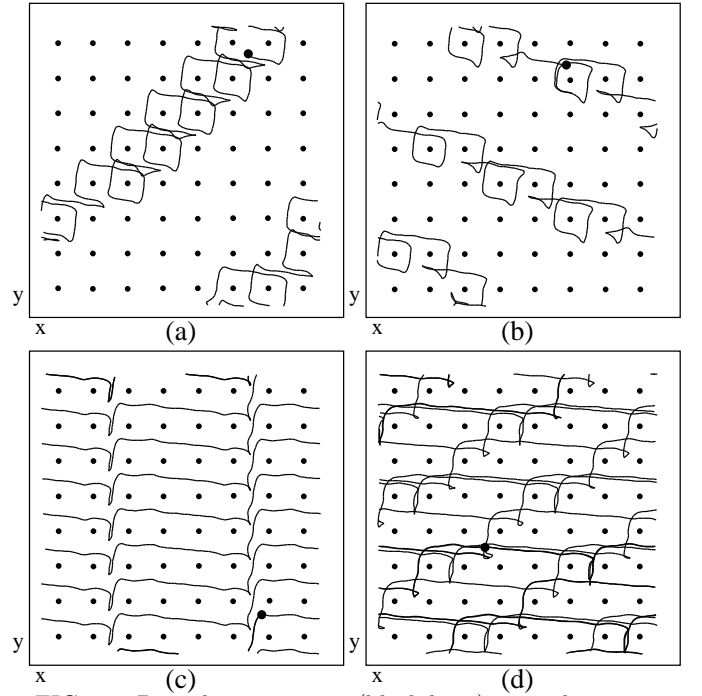


FIG. 12. Particle trajectories (black lines), periodic potential maxima (black dots), and driven particle (large dot) showing fractional rectifying orbits from the system in Fig. 9 for  $A = 0.325$  and  $f_{dc} =$  (a) 0.0465, (b) 0.0688, (c) 0.215, and (d) 0.378.

in the  $x$ -direction and  $a$  in the  $y$ -direction during each cycle. In Fig. 11(b) we show the orbit for  $f_{dc} = 0.21$  for the  $n = 3$  to  $n = 4$  transition, where the particle moves  $3a$  in the  $x$ -direction in a single cycle. In Fig. 11(c), near the  $n = 4$  to  $n = 5$  transition for  $f_{dc} = 0.29$ , the particle moves  $4a$  in the direction of drive during every cycle. The loop feature that occurs just before the particle translates a distance  $a$  in the  $y$ -direction becomes smaller with increasing step number. In Fig. 11(d), we show negative rectification for  $f_{dc} = 0.42$ , where the particle moves  $6a$  in the  $x$  direction and  $-a$  in the  $y$ -direction in a single period. Here the loop feature seen for the positive rectification orbits is lost and is replaced by a kink feature.

In Fig. 12 we show several examples of fractional rectifying orbits for  $A = 0.325$ . Figure 12(a) illustrates the trajectories for the rectification at the  $n = 0$  (pinned) to  $n = 1$  step transition at  $f_{dc} = 0.0465$ . In this case, the particle moves  $2a$  in the  $x$ -direction and  $a$  in the positive  $y$  direction every *two* cycles. To achieve this, the particle moves  $a$  in the  $x$ -direction and on average  $a/2$  in the positive  $y$  direction in each cycle. In Fig. 12(b) we show the negative rectification regime near the  $n = 1$  to  $n = 2$  transition for  $f_{dc} = 0.0688$ . We find a similar motion as in Fig. 12(a). Every two cycles, the particle moves  $2a$  in the positive  $x$  direction. The orbit forms a complete loop around one potential maximum during the first cycle, followed by an incomplete loop in the next cycle, at the end of which the particle has translated down by  $a$ .



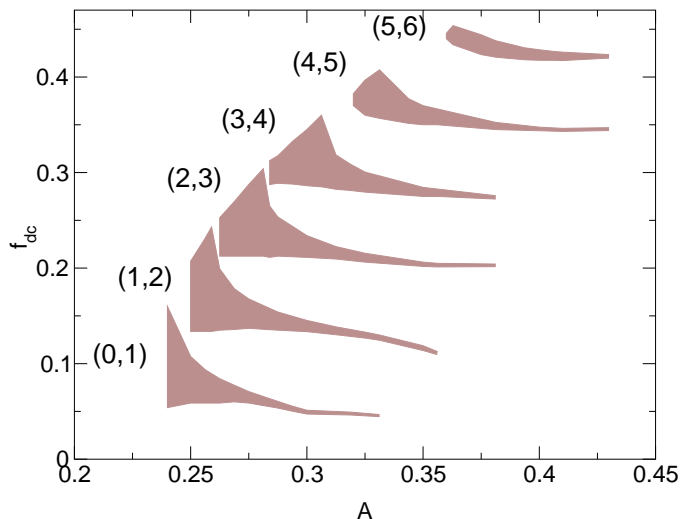


FIG. 13.  $f_{dc}$  vs  $A$ , where the shaded regions indicate positive integer rectifying regions obtained from Fig. 9.

Thus in a single period, the particle moves  $2a$  in the  $x$ -direction and an average of  $-a/2$  in the  $y$ -direction. We also find that at the onset of the integer rectifying phases, there can be a small region where the particle exhibits a fractional rectification. In Fig. 12(c) we show one such region that occurs at the end of the rectifying phase near the  $n = 3$  to  $n = 4$  transition for  $f_{dc} = 0.215$ . Here, in a single period the particle moves  $4a$  in the  $x$  direction, while it translates by  $a$  in the  $y$  direction every other cycle. During the first cycle, the trajectory dips down and up but the particle does not translate to the next upper row. On the following cycle, a cusp forms and the particle moves up to the next row. There are also several regimes for large  $A$  where the particle orbits rectify but do not repeat. For  $A = 0.325$  in Fig. 9, such a regime occurs near  $f_{dc} = 0.378$ . In Fig. 12(d) we plot the disordered orbit that occurs in this regime, showing that it has a net drift in the  $y$ -direction. We have also examined the rectifying orbits for other values of  $A$  and find that they are similar to those shown in Fig. 11 and Fig. 12.

### B. Rectification Phase Diagram

In Fig. 13 we plot  $f_{dc}$  vs  $A$ , and indicate the occurrence of integer rectification in the positive  $y$  direction by shaded regions. The phase diagram has the form of a series of tongues, where the width of any given rectifying phase decreases for increasing  $A$ . A larger number of rectifying phases appear at higher dc drive for increasing  $A$ , as seen from the rising envelope which begins at  $f_{dc} = 0.25$ . The rectifying phases for  $f_{dc} > 0.25$  increase in width with  $A$  over a small range of  $A$  before reaching a maximum width and then decreasing in width with increasing  $A$ . We do not have the resolution to determine

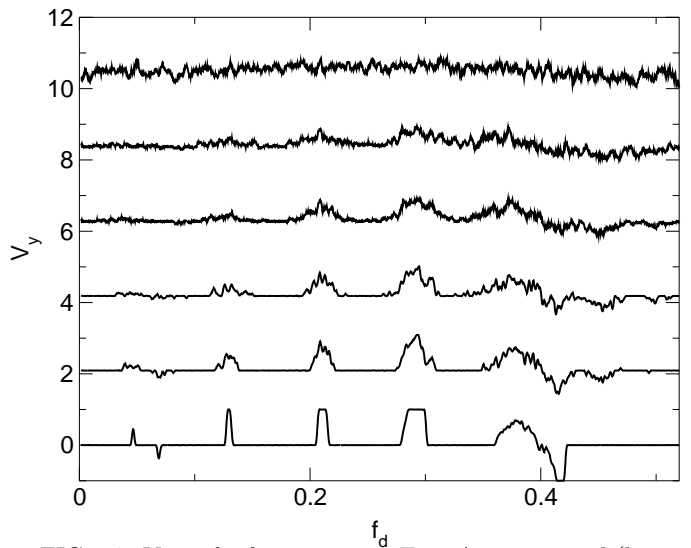


FIG. 14.  $V_y$  vs  $f_{dc}$  for increasing  $T$  at  $A = 0.325$  and (bottom to top)  $T = 0.0, 0.025, 0.0625, 0.1225, 0.5,$  and  $1.0$ . The curves have been shifted in the  $y$  direction for clarity.

whether the rectifying phases persist with continually decreasing width for higher ac amplitudes, or whether they actually terminate. We note that for  $A > 0.44$ , above the  $f_{dc} = 0$  transition from the orbit encircling one to encircling four maxima, a new set of rectifying phases appear at low  $f_{dc}$ , not shown in the figure.

We note that it is difficult to plot a phase diagram for the regions of negative rectification that occur for  $A > 0.35$ . Here the locking steps become hard to define due to the disordered regions where  $V_y$  does not settle down to a single value. In general, the negative rectification regimes show similar features to the positive rectification regions, with the width of the rectifying regime growing to a maximum value and then decreasing for increasing  $A$ . The phases also shift to higher  $f_{dc}$  for increasing  $A$ .

## VI. EFFECTS OF DISORDER

### A. Thermal Disorder

In many experimentally realizable systems such as colloids or biomolecules, thermal effects or Brownian motion are relevant. To model thermal effects, we add a noise term  $f^T$  to the equation of motion, with the properties  $\langle f^T(t) \rangle = 0.0$  and  $\langle f^T(t) f^T(t') \rangle = 2\eta k_B \delta(t-t')$ . We have performed a series of simulations for  $A = 0.3$  for different values of temperature. In Fig. 14 we show  $V_y$  vs  $f_{dc}$  for  $A = 0.325$  for increasing temperature. For low  $T$  there are still regions of  $V_y \approx 0$  within our resolution. The particle orbit at low temperatures shows only small perturbations, so the behavior is thermally activated and  $V_y$  is not strictly zero but instead is exponentially small. For higher  $T$ , the orbits are strongly perturbed, and the maximum value of  $V_y$  decreases while the width of the

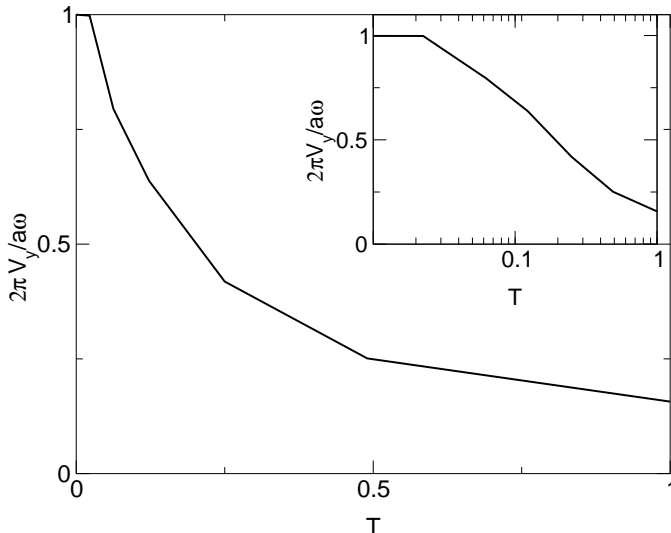


FIG. 15.  $2\pi V_y/a\omega$  vs  $T$  for  $A = 0.325$  and fixed  $f_{dc} = 0.29$ . The inset is a log-linear plot of the main figure.

rectifying regimes increases. For the highest temperatures, the particle diffuses rapidly; however, some rectification still occurs. For the top curve ( $T = 1$ ) there is only a slight positive rectification for  $f_{dc} < 0.4$ . As  $T$  increases further the rectification is gradually completely lost. In Fig. 15 we plot the average  $V_y$  for the positive rectification region at  $f_{dc} = 0.29$  for the bottom curve in Fig. 14 at  $T = 0.0$ . We define the temperature scale such that at  $T = 1.0$ , a single particle with  $f_{dc} = 0.0$  begins to diffuse, indicating that  $T = 1$  is the melting temperature for our parameters. In our system we have only one colloid, so thermal activation occurs at a much lower temperature than for a collection of interacting colloids. Fig. 15 shows a decay of  $V_y$  with increasing  $T$ , as illustrated more clearly in the inset. A reliable fit can be applied, giving  $2\pi V_y(T)/a\omega = (1 - \exp(-B/T))$ , which indicates thermal activation. The temperature scale can be changed by increasing the depth of the periodic wells as well as by the addition of other particles, which alters the effects of fluctuations.

## B. Particle Interactions

In many experimentally relevant systems it is likely that multiple particles would be moving through the array at the same time. If the density of the particles is sufficiently high, particle-particle interactions or scattering become relevant. For low fillings where the particles are still far apart, the  $V_y$  curves are only weakly perturbed. As the filling fraction is increased, the  $V_y$  curves exhibit some disordering. There are certain higher filling fractions such as  $1/16$  where the  $V_y$  curve is virtually identical to the single particle case. This is due to a commensuration effect. For particles with long range interactions such as vortices in superconductors or colloids

which are weakly screened, commensuration effects will occur for different particle densities. For fillings such as  $1/2$  where there is one mobile particle for every other plaquette, the particles form an ordered arrangement. In the case of half filling, the particles form a checkerboard state. Similar ordered states occur at fillings of  $1/16$ ,  $1/8$ ,  $1/5$ , and  $1/4$ . Since the arrangements are symmetrical at these fillings, the interactions effectively cancel and the system shows the same behavior as the single particle case. At incommensurate fillings where ordered particle arrangements cannot be formed, the particle-particle interactions become relevant.

## VII. SIMPLE MODEL SYSTEM

Let us return to the quantization of the velocity discussed above, and consider both the stable plateaus and the intermittent transitions between plateaus using general properties of nonlinear maps. Define a map  $(x, y) \rightarrow (x' + n_x a, y' + n_y a)$ , from the position of the particle at the start of a period to that at the end, where we may restrict to  $0 \leq x, y, x', y' \leq a$ , with  $n_x, n_y$  integer. Here, we have taken  $x, y, x', y'$  to indicate positions of the particle within a unit cell, while  $n_x, n_y$  indicate which unit cell the particle occupies after one orbit. We have fixed the unit cell of the particle at the start of the orbit; by translation symmetry, it does not matter which cell this is. If there is a stable fixed point,  $(x, y) = (x', y')$ , then the particle translates by  $(n_x a, n_y a)$  in time  $2\pi\omega^{-1}$  and so has average velocity  $V_x, V_y$  quantized in multiples of  $a\omega/(2\pi)$ , as found above. If the  $q$ -th power of the map has a stable fixed point, there are instead steps of fractional heights  $(p/q)a\omega$ .

As  $f_{dc}$  increases, the periodic orbit becomes unstable, and a different periodic orbit with larger  $V_x$  appears. This new orbit will be the next stable periodic orbit at higher drive. The transition to the new orbit can occur in one of three ways. (1) If both periodic orbits are stable simultaneously, the particle velocity will depend on the initial conditions in the transition regime. This was not observed. (2) The second periodic orbit could become stable at the same time that the first orbit becomes unstable. This behavior, which gives rise to infinitely sharp jumps in  $V_x$ , is not generic and hence not expected. (3) There can be a finite range of drive containing no stable periodic orbits. Over this range, the average velocity is not quantized. If, however, some orbits are close to stable, the particle will spend long times in these orbits, giving rise to intermittent behavior. This last behavior is consistent with what we observe.

The stability of the orbits is shown by the fact that in the middle of the plateaus the system is not sensitive to initial conditions, and by the exponentially small change in velocity at non-zero temperature. Outside the plateaus, the change in average velocity most likely will

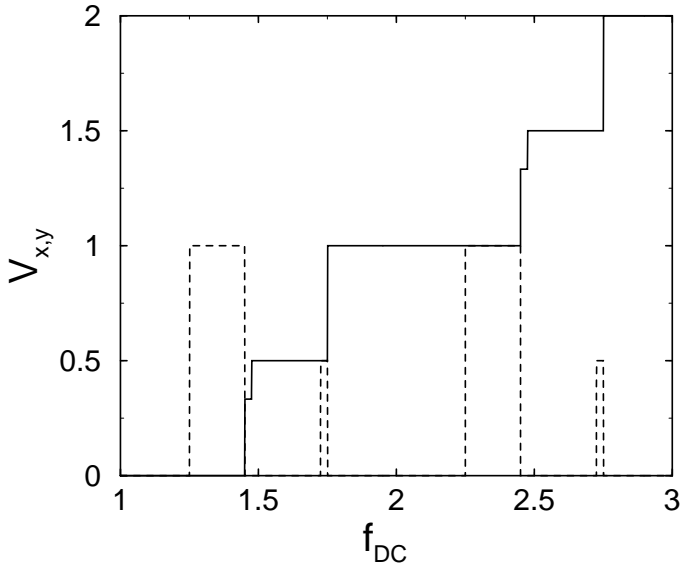


FIG. 16. Time averaged  $V_x$  (solid line) and  $V_y$  (dashed line) as a function of  $f_{dc}$  in toy model I.

not show a thermally activated form. We were not able to accurately measure the velocity in these reasons well enough to determine the temperature dependence of the velocity.

We now turn to a specific toy model illustrating some of these ideas. Consider a particle in a lattice of repulsive sites with  $a = 1$ , where the potential minima between repulsive sites are at integer  $x$  and  $y$  values. The  $y$  position of the particle is constrained to take only integer values, but the  $x$  position can be any real value. To model the translation of the particle through the lattice, we separate the  $x$  and  $y$  motion, so that the particle moves first (i.) right at velocity  $v_r$ , then (ii.) down, then (iii.) left at velocity  $v_l$ , then (iv.) up. In some cases, steps (ii.) and (iv.) of the cycle may not produce a change in  $y$  due to the constraint that  $y$  can be only integer valued; this corresponds to the confinement of the particle to a single row in the physical system. We consider two slightly different versions of the model. The first version, I, follows the following sequence of transitions: I(i.): We apply the rule  $x \rightarrow x + v_r$ . I(ii.): If  $x$  is within 0.25 of an integer,  $x$  is set to that integer and  $y$  is decremented by one. I(iii.): Apply  $x \rightarrow x - v_l$ . I(iv.): As in (ii.) except  $y$  is incremented by one. Here  $v_r$  and  $v_l$  are the velocity of the particle in the rightward and leftward parts of the cycle, respectively. In steps I(ii.) and I(iv.), the particle will *only* move to a new  $y$  position if it reaches the minima between sites at the correct phase of the driving period, when transverse motion is possible. In this case, the particle slips into the next row and the  $x$  coordinate of the particle is set to an integer value. In Fig. 16 we show the time-averaged velocities  $V_x$  and  $V_y$  obtained with model I for fixed  $v_l = 1.2$  and increasing  $v_r$ , representing increasing  $f_{dc}$ . It is clear that this simple model produces plateaus in  $V_x$  as well as ratcheting

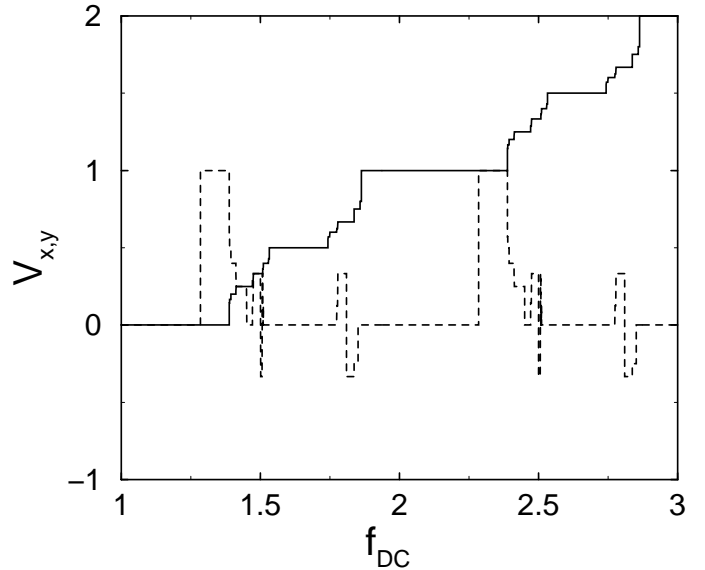


FIG. 17. Time averaged  $V_x$  (solid line) and  $V_y$  (dashed line) as a function of  $f_{dc}$  in toy model II.

behavior in  $V_y$ . The sharp jumps in the velocity values are due to the discontinuity of the map function, as in case (2) above; for smoother map functions, these jumps acquire a small but finite width. More complicated maps produce richer behavior, including occasional regimes of negative  $V_y$ . To show this, we consider a slightly different version of the model. In this model II, if the  $x$ -position of the particle is within a distance of 0.25 of an integer in step II(ii.) or II(iv.), the  $x$ -position is set equal to 0.25 times the present  $x$ -position plus 0.75 times the given integer. This smoother map allows a much richer behavior; if the particle is within 0.25 of an integer in the model I, the final position of the map does not depend on exactly where the particle position is near the given integer, while in model II the final position *does* depend on the precise particle position. We show the average velocities for this model in Fig. 17.

The ratcheting behavior in both the model and simulations occurs near transitions in  $V_x$  when the number of pinning centers the particle passes in one period changes, making it possible for the particle to interact asymmetrically with the pinning sites. For a clockwise orbit, the particle moves rapidly on the upper portion of the orbit, and is likely to scatter off the pinning site below when the orbit does not quite match  $na$ . On the lower part of the orbit, however, the particle is moving more slowly, and is likely to slip between the pinning sites above in spite of a small mismatch. The particle thus tends to ratchet in the positive  $y$  direction. If the dc drive is reversed, downward motion should be preferred, as we observe.

Finally, we note that much of this behavior is specific to two or more dimensions, or to systems in one dimension which are not overdamped so that both position and momentum are independent degrees of freedom.

Consider a map  $x \rightarrow x'$ , subject to  $x + a \rightarrow x' + a$  and  $dx'/dx \geq 0$ , true for overdamped motion in one dimension. It can then be shown that it is not possible to have periodic orbits with different values of the velocity as follows: Suppose there were two such orbits. Then, let initial conditions for the two orbits be  $x_1$  and  $x_2$ , and let the orbit starting at  $x_1$  have a greater velocity than that starting at  $x_2$ . Suppose that  $x_1 < x_2$  (this can always be accomplished by translating  $x_1$  by some number of unit cells); then, after some number of mappings,  $f(f(\dots(x_1)\dots)) > f(f(\dots(x_2)\dots))$ , which violates the assumption that  $dx'/dx \geq 0$ . Thus, all periodic orbits must have the same value of the velocity. Systems with Shapiro steps do not exhibit jumps.

### VIII. DISCUSSION

We now consider physical systems where the phase locking and the rectification might be realized. One possibility is colloids moving through a periodic 2D array. The array can be constructed from a substrate of hard obstacles or more smoothly varying objects. If the colloids are charged they can be driven with dc and ac electric fields. The most promising approach would be to use periodic arrays of optical traps [33–36] or dynamical optical trap arrays [11,13]. In this case colloids can be trapped at individual spots of laser light. Once the array is filled, additional colloids move through the periodic potential created by the pinned colloids. One advantage of the light arrays is that the array itself can be rotated dynamically to mimic ac driving when only an external dc force is applied. Recent experiments [12] have demonstrated the flow of colloids in 2D through periodic optical trap arrays. Another system would be vortices in superconductors driven with ac and dc currents. Periodic arrays of pinning sites can be lithographically constructed [37,38]. With the application of a magnetic field, flux enters in the form of quantized vortices. If the pinning sites are small enough that only a single vortex can be trapped at each site, then beyond the first matching field additional vortices will sit in the interstitial regions. It should also be possible to create arrays of anti-pinning sites, such as with an array of magnetic dots that are magnetized in the same direction as the applied field and create fixed vortices. Additional vortices created by the external field will move in the interstitial regions between the fixed vortices. These effects may also occur for fluxons in 2D Josephson junction arrays driven with a dc drive and a circular ac drive. In this case the fluxon can be viewed as a classical particle moving over a 2D periodic potential.

### IX. SUMMARY

To summarize, we have investigated the dynamics of overdamped particles moving in a 2D symmetrical periodic array where the particles are driven with a dc drive in the longitudinal direction and a circular ac drive. For small ac drives, we observe phase locking in the form of steps in the longitudinal velocity when the frequency of the ac drive matches with the frequency of the internally generated ac velocity component. For ac drives large enough that the particle can encircle at least one potential maximum at zero dc drive, we find phase locking steps in the longitudinal velocity for increasing dc drive. Additionally, in this regime we observe a non-zero transverse velocity in either the positive or negative direction in spite of the fact that there is no dc transverse applied drive. This rectification in the transverse direction arises due to the symmetry breaking caused by the circular ac drive. We propose and examine a more simplified model of the system that reproduces many of these features that we observe. The results of the simple model suggest that the phase locking and rectification phenomena described here are a general feature of a wide class of similar systems. We show that stable particle orbits occur along the longitudinal and transverse steps, while more chaotic orbits appear in non-step regions. Finally, we show that thermal disorder and incommensuration can smear or reduce the step size, but regions of rectification still occur. Our results should be testable for dc and driven vortex motion and colloids through 2D periodic arrays.

Acknowledgments—We thank C. Bechinger, M. Chertkov, D.G. Grier, P.T. Korda, and Z. Toroczkai for useful discussions. This work was supported by the US DOE under Contract No. W-7405-ENG-36.

- 
- [1] For a review of ratchet systems see: P. Reimann, Phys. Rep. **361**, 57 (2002); R.D. Astumian and P. Hänggi, Physics Today, **55**, 33 (2002).
  - [2] M. Magnasco, Phys. Rev. Lett. **71**, 1477 (1993); R.D. Astumian and M. Bier, *ibid.* **72**, 1766 (1994); C.R. Doering, W. Horsthemke, and J. Riordan, *ibid.* **72**, 2984 (1994); J. Rousselet, L. Salmoe, A. Adjari, and J. Prost, Nature (London) **370**, 446 (1994); R.D. Astumian, Science **276**, 917 (1997); F. Jülicher, A. Ajdari, and J. Prost, Rev. Mod. Phys. **69**, 1269 (1997).
  - [3] R. Bartussek, P. Hänggi, and J.C. Kissner, Europhys. Lett. **28**, 459 (1994); P. Jung, J.G. Kissner, and P. Hänggi, Phys. Rev. Lett. **76**, 3436 (1996); J.L. Mateos, *ibid.* **84**, 258 (2000).
  - [4] C. Mennerat-Robilliard, D. Lucas, S. Guibal, J. Tabosa, C. Jurczak, J.-Y. Courtois, and G. Grynberg, Phys. Rev. Lett. **82**, 851 (1999).

- [5] H. Linke, T.E. Humphrey, A. Lofgren, A.O. Sushkov, R. Newbury, R.P. Taylor, and P. Omling, *Science* **286**, 2314 (1999); M. Stopa, *Phys. Rev. Lett.* **88**, 146802 (2002).
- [6] Z. Farkas, P. Tegzes, A. Vukics, and T. Vicsek, *Phys. Rev. E* **60**, 7022 (1999); D.C. Rapaport, *Phys. Rev. E* **64**, 061304 (2001); J.F. Wambaugh, C. Reichhardt, and C.J. Olson, *Phys. Rev. E* **65**, 031308 (2002).
- [7] C.S. Lee, B. Jankó, I. Derenyi, and A.L. Barabasi, *Nature (London)* **400**, 337 (1999); J.F. Wambaugh, C. Reichhardt, C.J. Olson, F. Marchesoni, and F. Nori, *Phys. Rev. Lett.* **83**, 5106 (1999); C.J. Olson, C. Reichhardt, B. Jankó, and F. Nori, *ibid.* **87**, 177002 (2001); M.B. Hastings, C.J. Olson Reichhardt, and C. Reichhardt, *ibid.* **90**, 247004 (2003).
- [8] I. Zapata, R. Bartussek, F. Sols, and P. Hänggi, *Phys. Rev. Lett.* **77**, 2292 (1996); S. Weiss, D. Koelle, J. Muller, R. Gross, and K. Barthel, *Europhys. Lett.* **51**, 499 (2000); E. Goldobin, A. Sterck, and D. Koelle, *Phys. Rev. E* **63**, 031111 (2001); G. Carpella, *Phys. Rev. B* **63**, 054515 (2001); G. Carapella and G. Costabile, *Phys. Rev. Lett.* **87**, 077002 (2001); P.D. Shaju and V.C. Kuriakose, *Phys. Lett. A* **299**, 628 (2002).
- [9] W.D. Volkmuth and R.H. Austin, *Nature (London)* **358**, 600 (1992); T.A.J. Duke and R.H. Austin, *Phys. Rev. Lett.* **80**, 1552 (1998); D. Ertas, *ibid.* **80**, 1548 (1998); A. Oudenaarden and S.G. Boxer, *Science* **285**, 1046 (1999); C.F. Chou, O. Bakajin, S.W.P. Turner, T.A.J. Duke, S.S. Chan, E.C. Cox, H.G. Craighead, and R.H. Austin, *Proc. Natl. Acad. Sci. U.S.A.* **96**, 13762 (1999); C.-F. Chou, R.H. Austin, O. Bakajin, J.O. Tegenfeldt, J.A. Castellino, S.S. Chan, E.C. Cox, H. Craighead, N. Darnton, T. Duke, J.Y. Han, and S. Turner, *Electrophoresis* **21**, 81 (2000); L.R. Huang, P. Silberzan, J.O. Tegenfeldt, E.C. Cox, J.C. Sturm, R.H. Austin, and H. Craighead, *Phys. Rev. Lett.* **89**, 178301 (2002).
- [10] J.L. Viovy, *Rev. Mod. Phys.* **72**, 813 (2000).
- [11] C. Reichhardt and F. Nori, *Phys. Rev. Lett.* **82**, 414 (1999); J. Wiersig and K.H. Ahn, *Phys. Rev. Lett.* **87**, 026803 (2001).
- [12] P.T. Korda, M.B. Taylor, and D.G. Grier, *Phys. Rev. Lett.* **89**, 128301 (2002); K. Ladavac, K. Kasza, and D.G. Grier, *cond-mat/03210396*; M.P. MacDonald, G.C. Spalding, and K. Dholakia, *Nature (London)* **426**, 421 (2003).
- [13] For a review of optical manipulation of colloids see: D.G. Grier, *Nature* **424**, 810 (2003).
- [14] G.A. Cecchi and M.O. Magnasco, *Phys. Rev. Lett.* **76**, 1968 (1996).
- [15] R. Eichhorn, P. Reimann, and P. Hänggi, *Phys. Rev. Lett.* **88**, 228305 (2002).
- [16] Z. Zheng, M.C. Cross, and G. Hu, *Phys. Rev. Lett.* **89**, 154102 (2002).
- [17] O. Usmani, E. Lutz, and M. Nuttiker, *Phys. Rev. E* **66**, 021111 (2002); R. Guantes and S. Miret-Artes, *ibid.* **67**, 046212 (2003).
- [18] S. Shapiro, *Phys. Rev. Lett.* **11**, 80 (1963); A. Barone and G. Paterno, *Physics and Applications of the Josephson Effect* (Wiley, New York, 1982); S.P. Benz, M.S. Rzchowski, M. Tinkham, and C.J. Lobb, *Phys. Rev. Lett.* **64**, 693 (1990).
- [19] G. Grüner, *Rev. Mod. Phys.* **60**, 1129 (1988); R.E. Thorne, *Physics Today*, **49**, No. 5, 42 (1996).
- [20] P. Martinoli, O. Daldini, C. Leemann, and E. Stocker, *Sol. St. Commun.* **17**, 205 (1975).
- [21] L. Van Look, E. Rosseel, M.J. Van Bael, K. Temst, V.V. Moshchalkov, and Y. Bruynseraede, *Phys. Rev. B* **60**, R6998 (1999).
- [22] C. Reichhardt, R.T. Scalettar, G.T. Zimányi, and N. Grønbech-Jensen, *Phys. Rev. B* **61**, R11 914 (2000).
- [23] C. Reichhardt, A.B. Kolton, D. Domínguez, and N. Grønbech-Jensen, *Phys. Rev. B* **64**, 134508 (2001); C. Reichhardt and C.J. Olson, *ibid.* **65**, 174523 (2002); V.I. Marconi, A.B. Kolton, D. Domínguez, and N. Grønbech-Jensen, *ibid.* **68**, 104521 (2003).
- [24] A.T. Fiory, *Phys. Rev. Lett.* **27**, 501 (1971); J.M. Harris, N.P. Ong, R. Gagnon, and L. Taillefer, *ibid.* **74**, 3684 (1995).
- [25] A.B. Kolton, D. Domínguez, and N. Grønbech-Jensen, *Phys. Rev. Lett.* **86**, 4112 (2001).
- [26] N. Kokubo, R. Besseling, V.M. Vinokur, and P.H. Kes, *Phys. Rev. Lett.* **88**, 247004 (2002).
- [27] A.B. Kolton, D. Domínguez, and N. Grønbech-Jensen, *Phys. Rev. B* **65**, 184508 (2002).
- [28] C. Reichhardt, C.J. Olson, and M.B. Hastings, *Phys. Rev. Lett.* **89**, 024101 (2002).
- [29] C. Reichhardt and C.J. Olson Reichhardt, *Phys. Rev. E* **68**, 046102 (2003).
- [30] D. Weiss, M.L. Roukes, A. Menshig, P. Grambow, K. von Klitzing, and G. Weimann, *Phys. Rev. Lett.* **66**, 2790 (1991); R. Fleischmann, T. Geisel and R. Ketzmerick, *ibid.* **68**, 1367 (1992).
- [31] C. Reichhardt and C.J. Olson, *Phys. Rev. B* **65**, 100501(R) (2002).
- [32] C. Reichhardt and C.J. Olson Reichhardt, *cond-mat/0311489*.
- [33] M. Brunner and C. Bechinger, *Phys. Rev. Lett.* **88**, 248302 (2002); K. Dholakia, G.C. Spalding, and M.P. MacDonald, *Physics World*, **15**, 31 (2002); K. Mangold, P. Leiderer, and C. Bechinger, *Phys. Rev. Lett.* **90**, 158302 (2003).
- [34] E.R. Dufresne and D.G. Grier, *Rev. Sci. Instrum.* **69**, 1974 (1998); E.R. Dufresne, G.C. Spalding, M.T. Dearing, S.A. Sheets, and D.G. Grier, *Rev. Sci. Instrum.* **72**, 1810 (2001).
- [35] M. Brunner and C. Bechinger, *Phys. Rev. Lett.* **88**, 248302 (2002).
- [36] P.T. Korda, G.C. Spalding, and D.G. Grier, *Phys. Rev. B* **66**, 024504 (2002).
- [37] A.T. Fiory, A.F. Hebard, and S. Somekh, *Appl. Phys. Lett.* **32**, 73 (1978); M. Baert, V.V. Metlushko, R. Jonckheere, V.V. Moshchalkov, and Y. Bruynseraede, *Phys. Rev. Lett.* **74**, 3269 (1995); K. Harada, O. Kamimura, H. Kasai, T. Matsuda, A. Tonomura, and V.V. Moshchalkov, *Science* **274**, 1167 (1996); A.N. Grigorenko, G.D. Howells, S.J. Bending, J. Bekaert, M.J. Van Bael, L. Van Look, V.V. Moshchalkov, Y. Bruynseraede, G. Borghs, I.I. Kaya, and R.A. Stradling, *Phys. Rev. B* **63**, 052504 (2001); S.B. Field, S.S. James, J. Barentine, V. Metlushko, G. Crabtree, H. Shtrikman, B. Ilic, and S.R.J. Brueck, *Phys. Rev. Lett.* **88**, 067003 (2002).

- [38] D.J. Morgan and J.B. Ketterson, Phys. Rev. Lett. **80**, 3614 (1998); J.I. Martín, M. Vélez, A. Hoffmann, I.K. Schuller, and J.L. Vicent, Phys. Rev. Lett. **83**, 1022 (1999); Y. Fasano, M. Menghini, F. de la Cruz, and G. Nieva, Phys. Rev. B **62**, 15183 (2000); M.J. Van Bael, J. Bekaert, K. Temst, L. Van Look, V.V. Moshchalkov, Y. Bruynseraede, G.D. Howells, A.N. Grigorenko, S.J. Bending, and G. Borghs, Phys. Rev. Lett. **86**, 155 (2001).